

# INTERFACIAL RHEOLOGY IN COMPLEX FLOW

**Jeffrey D. Martin and Steven D. Hudson**

*Complex Fluids Group, Polymers Division, National Institute of Standards and Technology  
100 Bureau Dr., Gaithersburg, MD 20899-8542*

**Abstract:** Typical methods used to measure dynamic interfacial properties of multiphase liquid systems often employ drops that are much larger and flows that are much simpler than those encountered in typical processing applications. A microfluidic approach is used here to measure dynamic structure and kinetics in multiphase systems with drop sizes comparable to those encountered in applications and flow complexity that is easily adjustable. The internal circulation and deformation of an isolated aqueous droplet in oil (paraffin and canola) is measured using particle tracers and a detailed shape analysis, which is capable of measuring sub- $\mu\text{m}$  deviations in drop shape. Deformation dynamics, detailed drop shape, interfacial tension, and internal circulation patterns and velocities are measured in Poiseuille and transient elongational flows. Mass transfer of surface active solutes has also been explored.

**Keywords:** microfluidics, multiphase flow, surfactant mass transfer, interfacial tension, drop size

## 1. INTRODUCTION

Multiphase liquid systems are ubiquitous in and essential to everyday life, e.g., foods, pharmaceuticals, cosmetics, paints, oil recovery, etc. The performance of such systems depends on dynamic interfacial properties and processes. Typical methods used to measure such interfacial properties often employ drops that are much larger and flows that are much simpler than those encountered in typical processing applications. A microfluidic approach is used here to measure dynamic structure and kinetics in multiphase systems with drop sizes comparable to those encountered in applications and with adjustable, complex flows more typical of processing applications. The internal circulation and deformation of an isolated aqueous droplet in clear mineral oil is measured using particle tracers and a detailed shape analysis, which is capable of measuring sub- $\mu\text{m}$  deviations in drop shape. Deformation dynamics, detailed drop shape, interfacial tension, and internal circulation patterns and velocities (indicative of interfacial mobility) are measured in Poiseuille and transient elongational flows. Mass transfer of surface active solutes has also been explored.

## 2. MATERIALS AND METHODS

Various fluids and additives were used in this study: heavy paraffin oil (Aldrich<sup>1</sup>), canola oil (from a local grocer), n-butanol (Mallinckrodt), sodium dodecyl sulphate (sds, Fluka), surfactant-free 2  $\mu\text{m}$  polystyrene particles, and distilled water were used. All were used as received. Aqueous solutions of butanol (1 %, 2 % and 5 % mass fraction) and an aqueous solution of sds (0.05 % mass fraction) were prepared.

Fabrication of the microfluidic device from poly(dimethylsiloxane) (PDMS, Dow Sylguard) gel has been described in detail previously (Cabral and Hudson 2006). A master channel mold was fabricated first from SU-8-2075

---

<sup>1</sup> Certain commercial materials and equipment are identified in this paper in order to adequately specify the experimental procedure. In no case does such identification imply recommendation or endorsement by the National Institute of Standards and Technology, nor does it imply that these are necessarily the best available for the purpose.

(MicroChem), and then replicated with PDMS. The PDMS device was exposed briefly to O<sub>2</sub> plasma, sealed onto a clean glass slide, fitted with tubing and connected to micro-stepping syringe pumps (New Era Pump Systems). The syringe diameters are known, so that the pumps deliver fluid volumes with accuracy better than 0.1 %. Aqueous drops are produced at a T-junction and four inputs for the continuous fluid are provided to easily tune the drop size, spacing and height (Cabral and Hudson 2006). The main channel of the device also contains several constrictions, where drops may stretch, if viscous forces are strong enough. The relative strength of Poiseuille and extensional flow are adjustable by channel geometry and drop size. Non-linearity of the shear flow is adjustable by drop height. The flow field in the channel was further explored by three-dimensional finite-element steady-state Navier-Stokes calculations (using approximately 10<sup>4</sup> tetrahedral elements in the Comsol Multiphysics 3.2 package).

Pumping and data acquisition are computer controlled (LabVIEW). 8-bit grayscale images (400 pixels x 1504 pixels) were acquired with a Redlake HG100k CMOS camera at 2 kHz. Image analyses (LabVIEW) of instantaneous drop center of mass, major and minor axes, and orientation were recorded in time. The temperature was also recorded and used to compute the fluid viscosities (Rabelo et al. 2000).

The dynamics of deformation and retraction of an isolated drop with uniform interfacial tension subject to an unbounded flow field are well established (Taylor 1934; Rallison 1984) and form a basis of interfacial tension metrology (Hudson et al. 2005; Cabral and Hudson 2006). As noted previously, the transient response of a drop may be plotted thus to yield the apparent tension  $\sigma$  from the slope.

$$\alpha \eta_c (5(\dot{\epsilon}_1 - \dot{\epsilon}_2)/(4\hat{\eta} + 6) - \dot{D}) = \sigma D/a_0 \quad (1)$$

The parameter  $\alpha$  is a weak function of viscosity ratio  $\hat{\eta}$  ( $=\eta_d/\eta_c$ ), and  $\eta_c$  is the continuous phase viscosity.  $\dot{\epsilon}_i$  are the principal extension rates,  $D$  is deformation (normalized difference of principal drop radii),  $dD/dt$  is its material derivative, and  $a_0$  is the drop radius. Numerical simulations of drop response to a strain rate impulse indicates that this apparent tension is accurate to 1 % if  $D < 0.02$  (Gonzalez-Mancera 2007). Marangoni effects, when present, can cause more significant deviations. While  $D$  is based merely on the principal radii of an equivalent ellipse, a full two-dimensional analysis of the drop interface (approximately 0.1 pixel accuracy) was also carried out. Furthermore, the internal drop circulation was measured by particle tracking of internal tracer particles.

### 3. RESULTS AND DISCUSSION

The behavior of isolated drops as they pass through the microchannel device was examined. For drops small compared to the height and width of the channel, the drop velocity  $u$  was nearly equal to the fluid velocity calculated on the same streamline (Fig. 1), as expected when the relative viscosity of the drop is near zero (Hetsronni et al. 1970). For surfactant-free drops near the centerline of the channel, the internal circulation velocity was found to be approximately  $2/\pi (2a/h)^2 u$ . The drop shape is nearly spherical. The largest distortions occur at the entrance and exit of the constriction (Fig. 1 b), where the acceleration is of greatest magnitude (Fig. 1a). Therefore, tracking the motion and shape of drops in this region is of particular interest. This perturbation is minor and short lived. Inertia is of little significance, since the maximum value of  $Re$  is 0.1. The apparent interfacial tension is obtained according to equation 1 from analysis of the entrance region (i.e.,  $x: [-2, -1]$ ), as shown in Fig. 1). At these locations, the drop is extended slightly and the interfacial tension can be measured. The passage time from the moment of drop formation to that of measurement of interfacial tension was determined using drop velocity measurements.

Based on such data, restricted to the entrance and  $D < 0.02$ , (Gonzalez-Mancera 2007) the apparent  $\sigma$  is measured as a function of  $a_0$ , interface age (droplet residence time) and input butanol (surfactant) concentration  $c(0)$  (Fig. 2). When  $c = 0$  (pure water/oil),  $\sigma$  is independent of  $a_0$ , drop spacing and total flow rate (interface age). However, when  $c(0) > 0$ ,  $\sigma$  became a function of  $a_0$ ,  $c(0)$  and interface age. As the interface ages,  $\sigma$  increases. However, Fig. 2b does not show the minimum in interfacial tension that is expected in such systems where there is surfactant mass transport across the liquid/liquid interface (Ferrari et al. 1997; Liggieri et al. 1997). This minimum is not observed here, since short interface age ( $< 1$  s) are not accessible in this device; extremely large flow rates are needed for short residence times. Similar behavior is observed with paraffin oil.

A convection-diffusion model was applied to estimate the concentration of butanol inside the drop as a function of interface age. Since the solute is convected in the oil from the neighborhood of one drop to that of the subsequent one more quickly than it diffuses from the drop, the phenomenon is effectively two-dimensional: diffusion is only

relevant transverse to the streamlines. To test this concept, the apparent tension was measured over a wide range of drop spacing and found to be constant. We also assume that convection (observed internal circulation) homogenizes the concentration inside the drop. Diffusion from a finite uniform cylindrical source gives the following time dependent source concentration (Crank 1975).

$$c(t)/c(0) = \left(1 + 2\sqrt{\mathcal{D}t}/a + 3\mathcal{D}t/a^2\right)^{-1} \quad (2)$$

The characteristic timescale of this mass transfer process is  $a^2/\mathcal{D}$  (of the order of a few seconds), where  $\mathcal{D}$  denotes diffusivity. By varying drop sizes and interface ages, the adsorption isotherm can be constructed (Fig. 2b).

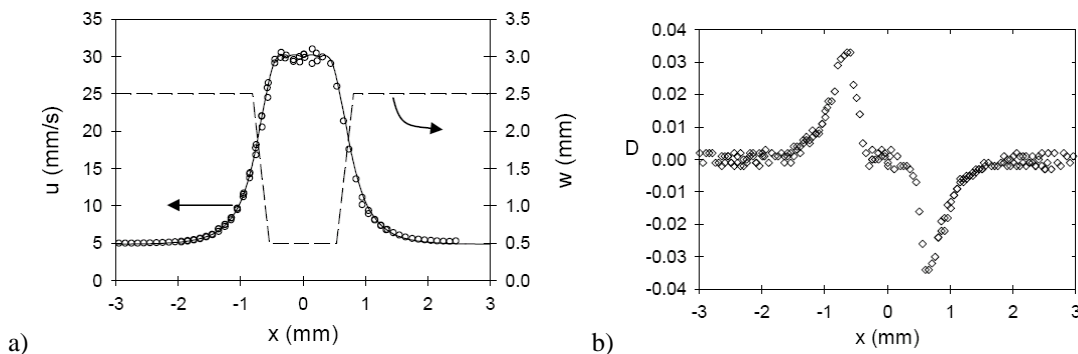


Fig. 1. Drop velocity (a) and deformation (b) as a drop passes through a constriction in the channel. The channel width profile  $w$  is plotted in (a) with dashed lines. The channel height is  $496 \mu\text{m}$ . Data points signify measurements (whose statistical uncertainty is illustrated by their scatter) and the solid curve (in a) is a finite element calculation of the centerline velocity. Total volumetric flow rates in (a) and (b) are  $12.82 \text{ mL/h}$  and  $10.82 \text{ mL/h}$ , respectively, while the drop radius is  $54 \mu\text{m} \pm 2 \mu\text{m}$ .

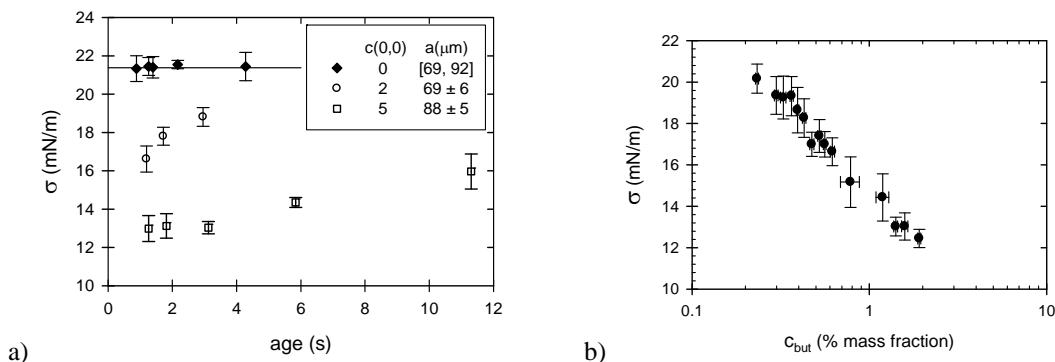


Fig. 2. a.) Measured interfacial tension  $\sigma$  vs. interface age. Initial n-butanol concentration  $c(0)$  and average drop radii  $a$  are listed in the legend. Standard uncertainties are reported. b.) Measured interfacial tension  $\sigma$  vs. estimated n-butanol concentration.

#### 4. CONCLUSIONS

These measurements, analysis and modeling of decaying interfacial pressure demonstrate quantitative detection of the kinetics of release of a surface-active solute diffusing from a drop in two-phase flow, accounting for convection inside and outside the drop. The ability to adjust drop size here provides access to a range of dimensionless interface age. This ability to tune drop size and that of scaling the device channel and drop dimensions is valuable for future studies of interfacial kinetics of surfactants during flow.

## REFERENCES

- Cabral, J. T. and S. D. Hudson (2006). "Microfluidic approach for rapid multicomponent interfacial tensiometry." *Lab On a Chip* **6**(3): 427-436.
- Crank, J. (1975). The mathematics of diffusion. Oxford, Clarendon Press.
- Gonzalez-Mancera, A. (2007). Effects of non-linear interfacial mechanics on the transient response of a drop to an external flow field. Mechanical Engineering. Baltimore, MD, University of Maryland, Baltimore County. **Ph.D.:** 124.
- Hetsronni, G., S. Haber, et al. (1970). "The flow field in and around a droplet moving axially within a tube." *J.Fluid Mech.* **41** 689.
- Hudson, S. D., J. T. Cabral, et al. (2005). "Microfluidic interfacial tensiometry." *Applied Physics Letters* **87**: 081905.
- Rabelo, J., E. Batista, et al. (2000). "Viscosity prediction for fatty systems." *Journal of the American Oil Chemists Society* **77**(12): 1255-1261.
- Rallison, J. M. (1984). "The deformation of small viscous drops and bubbles in shear flows." *Ann.Rev.Fluid Mech.* **16**: 45-66.
- Taylor, G. I. (1934). "The Formation of Emulsion in Definable Fields of Flow." *Proc.R.Soc.Lond.A* **146**: 501-523.